



Searches for $t\bar{t}$ resonances in ATLAS

Reina Coromoto Camacho Toro

► **To cite this version:**

Reina Coromoto Camacho Toro. Searches for $t\bar{t}$ resonances in ATLAS. Beyond The Standard Model of Particle Physics, Jul 2012, Qui Nhon, Vietnam. in2p3-00760281

HAL Id: in2p3-00760281

<http://hal.in2p3.fr/in2p3-00760281>

Submitted on 3 Dec 2012

HAL is a multi-disciplinary open access archive for the deposit and dissemination of scientific research documents, whether they are published or not. The documents may come from teaching and research institutions in France or abroad, or from public or private research centers.

L'archive ouverte pluridisciplinaire **HAL**, est destinée au dépôt et à la diffusion de documents scientifiques de niveau recherche, publiés ou non, émanant des établissements d'enseignement et de recherche français ou étrangers, des laboratoires publics ou privés.

SEARCHES FOR $t\bar{t}$ RESONANCES IN ATLAS

REINA CAMACHO TORO

*Laboratoire de Physique Corpusculaire (LPC), Campus des Cézeaux. 24, Avenue des Landais BP
80026. 63171 Aubière Cedex, France.*

E-mail: reina.coromoto.camacho.toro@cern.ch

On behalf of the ATLAS collaboration

A search for $t\bar{t}$ resonances has been performed using 2.05 fb^{-1} of pp collisions at $\sqrt{s} = 7 \text{ TeV}$ recorded by ATLAS in 2011. The dilepton, resolved lepton+jets and a boosted lepton+jets topology have been considered. No evidence of a resonance was found. Limits were set on the production cross-section times branching ratio to $t\bar{t}$ for narrow and wide resonances. The search excludes at 95% confidence level narrow leptophobic topcolor Z' bosons with masses between 500 and 1150 GeV and wider Kaluza-Klein gluons with masses between 500 and 1500 GeV.

1 Introduction

The top quark is the heaviest elementary particle known, with a mass close to the scale of electroweak symmetry breaking. The large top quark mass hints at an intimate connection between the top quark and beyond the Standard Model (BSM) physics. So far, searches for manifestations for such physics have remained unsuccessful, and such searches therefore continue to explore a wide spectrum of possible signatures. A promising approach are BSM theories predicting the existence of new heavy particles decaying into top quark pairs.

In the SM, the top quark decays approximately 99% of the time into a W boson and a b -quark. The top quark decay final states are determined by the decay of the W , which decays approximately 33% into a charged lepton-neutrino (leptonic decay) pair and 67% into a quark-antiquark pair (hadronic decay). If the lepton is a τ , it will decay subsequently into an electron/muon-neutrino pair or hadronically. This results in three decay topologies: **hadronic**, **lepton plus jets** and **dilepton**.

This report summarizes recent results of the search for new heavy particles decaying to $t\bar{t}$ pairs using the ATLAS detector¹ at the CERN Large Hadron Collider (LHC) in three different final state topologies: the dilepton channel², the resolved lepton plus jets channel^{2,3} and the boosted lepton plus jets channel⁴. The latter is increasingly important in searches for resonances with masses above 1 TeV where the hadronically decaying top quark daughters merge into one or two jets. Only final state topologies containing at least one electron or muon expected to come from the decay of one of the W bosons produced in the top quark decays are considered. All analyses use 2.05 fb^{-1} of data collected by ATLAS in the first half of 2011.

The benchmark model used to quantify the experimental sensitivity to narrow resonances is a leptophobic Z' boson arising in models of strong electroweak symmetry breaking through top quark condensation (specifically the leptophobic scenario known as Model IV⁵). The model used for wide resonances is a Kaluza-Klein (KK) gluon g_{KK} , which appears in Randall-Sundrum



(RS) models with one warped extra dimension^{6,7,8}. This model is taken as a proxy for coloured resonances. Previous searches for $t\bar{t}$ resonances recently carried out did not show evidence for new resonances and limits were set on the mass of a Z' boson excluding $m_{Z'} > 900$ GeV⁹ as well as placing upper limits on the coupling strengths of a heavy colour-octet vector particle.

2 Event selection

Events are selected using a single lepton trigger. Each event is required to have at least one offline-reconstructed primary vertex with at least five tracks, and it is discarded if any jet with $p_T > 20$ GeV is identified as out-of-time activity or calorimeter noise.

2.1 Dilepton channel

The event must contain exactly two isolated leptons of opposite charge. Electron candidates are required to have $p_T > 25$ GeV and $|\eta| < 2.47^a$, while muon candidates are required to have $p_T > 20$ GeV and $|\eta| < 2.5$. Two or more jets with $p_T > 25$ GeV and $|\eta| < 2.5$ are also required. Jets are reconstructed using the anti- k_t algorithm ($R = 0.4$)¹⁰ and calibrated using a correction factor obtained from simulation¹¹. To suppress the Z plus jets background, events are required to have $E_T^{\text{miss}} > 40$ GeV and an invariant dilepton mass not compatible with the Z boson mass range ($|m_Z - m_{ll}| > 10$ GeV) for ee and $\mu\mu$ events, where E_T^{miss} is the module of the missing transverse momentum in the event. In the $e\mu$ channel the non- $t\bar{t}$ background is suppressed by requiring the scalar sum of the transverse momenta of the leptons and jets, H_T , to be larger than 130 GeV.

2.2 Resolved lepton plus jets channel

The event must contain exactly one isolated lepton. Electrons must have $p_T > 25$ GeV and $|\eta| < 2.47$, while muons must have $p_T > 20$ GeV and $|\eta| < 2.5$. Events where an electron shares an inner detector track with a non-isolated muon or with a second lepton with $p_T > 15$ GeV are rejected. The total event fraction of $t\bar{t}$ is increased by applying the following event cuts: first, in the electron channel, $E_T^{\text{miss}} > 35$ GeV and $M_T(\text{lepton}, E_T^{\text{miss}}) > 25$ GeV, where $M_T(\text{lepton}, E_T^{\text{miss}})$ is the lepton- E_T^{miss} transverse mass. In the muon channel, $E_T^{\text{miss}} > 20$ GeV and $E_T^{\text{miss}} + M_T(\text{lepton}, E_T^{\text{miss}}) > 60$ GeV is required. Finally, the leading jet must have $p_T > 60$ GeV and the event must contain at least four jets with $p_T > 25$ GeV and $|\eta| < 2.5$, where at least one of the jets must be tagged as a b -quark jet using the MV1 algorithm¹². The jet multiplicity requirement is relaxed to at least three jets if one of the jets has jet mass $m_j > 60$ GeV, since for boosted top quarks two of the quark daughters from the hadronic top quark decay can be merged into a single jet. Jets are reconstructed using the anti- k_t algorithm ($R = 0.4$).

2.3 Boosted lepton plus jets channel

The lepton selection and multijet background rejection is similar to the one used in the lepton plus jets resolved channel. The jet selection is modified for the expected boosted topology. The lepton and the jet from the leptonic top quark decay are expected to be collimated, therefore a jet with $p_T > 30$ GeV and with an $\eta - \phi$ separation ΔR from the lepton candidate of $0.4 < \Delta R < 1.5$ of the selected lepton is required. The decay products from the hadronic top quark decay are

^aATLAS uses a right-handed coordinate system with its origin at the nominal interaction point (IP) in the centre of the detector and the z -axis along the beam pipe. The x -axis points from the IP to the centre of the LHC ring, and the y -axis points upward. Cylindrical coordinates (r, ϕ) are used in the transverse plane, ϕ being the azimuthal angle around the beam pipe. The pseudorapidity is defined in terms of the polar angle θ as $\eta = -\ln \tan(\theta/2)$.

expected to be merged into a single fat jet back-to-back to the leptonic top quark decay. Fat jet candidates are reconstructed using the anti- k_t algorithm with a distance parameter $R = 1.0$. Fat jets that potentially overlap with the jet associated with the leptonic top quark decay are not considered ($\Delta R(j, j) > 1.5$).

An analysis of the substructure of the fat jet can be used to increase the $t\bar{t}$ signal. To this end two observables are considered in this analysis. The first one is the jet mass, m_j , obtained by adding the four vectors of all jet constituents (topological clusters). The second one is the last splitting scale, $\sqrt{d_{12}}$ ¹³. Jet constituents are reclustered with the k_t algorithm and $\sqrt{d_{12}}$ represent the scale at which the fat jet would split into two, i.e the last step of the clustering sequence. For fat jets containing the hadronic decay of a boosted top quark is typically around the W -mass. Therefore, at least one fat jet must satisfy $\sqrt{d_{12}} > 40$ GeV, $p_T > 250$ GeV and $m_j > 100$ GeV. The leading fat jet is taken as the hadronic top quark candidate.

3 Backgrounds and signals

The irreducible SM $t\bar{t}$ and electroweak single top quark backgrounds are simulated using the MC@NLO generator^{14,15} interfaced to the HERWIG¹⁶ parton showering and hadronization model and the JIMMY¹⁷ underlying event model. In the dilepton channel, the small contribution of events with at least one fake lepton is estimated from data using the Matrix Method¹⁸ which accounts for small backgrounds with both one (W plus jets) and two fake leptons (multijet background). In the lepton plus jets channel, the W plus jets samples are simulated with the ALPGEN generator and they are normalized using data-driven techniques. In the lepton plus jets resolved channel, the multijet background is derived from a jet-triggered sample where exactly one jet is required with a high electromagnetic fraction. The full E_T^{miss} distribution of this sample and the simulated $t\bar{t}$, single top, W plus jets and Z plus jets background samples are fitted to the data to calculate its normalization. In the lepton plus jets boosted channel the Matrix Method is used to estimate the multijet background contribution. The Z plus jets events are simulated using the ALPGEN¹⁹ Monte Carlo. In the dilepton channel, this background is normalized in a data control sample orthogonal to the signal sample. Diboson WW , ZZ and WZ samples are produced using the HERWIG generator and JIMMY model.

Samples for topcolor Z' bosons were generated with the PYTHIA²⁰ Monte Carlo. Samples for KK gluons were generated with MADGRAPH²¹ showered with the PYTHIA Monte Carlo. Any interferences with SM processes were assumed to be negligible.

4 $t\bar{t}$ mass reconstruction

4.1 Dilepton channel

In the dilepton channel the $t\bar{t}$ mass reconstruction present ambiguities due to the presence of two neutrinos. The effective mass, defined as the scalar sum of $H_T + E_T^{\text{miss}}$, is used as the discriminating variable. Figure 1(c) shows the $H_T + E_T^{\text{miss}}$ distribution for data and SM expectation.

4.2 Resolved lepton plus jets channel

In this channel, the event E_T^{miss} corresponds to the neutrino's transverse momentum p_T and the neutrino's longitudinal momentum (p_z) is determined by imposing the W boson mass constraint. The leptonically decaying W boson candidate is reconstructed from the lepton and the reconstructed neutrino.

The $t\bar{t}$ pair is reconstructed differently depending on the highest mass jet in the event. For events where all jets have masses below 60 GeV, the $dRmin$ algorithm² is used to identify as

$t\bar{t}$ final state daughters those jets whose $\eta - \phi$ separation, ΔR , with the lepton or closest jet satisfies: $\Delta R > 2.5 - 0.015 \times m_j$. If a jet was discarded and more than three jets remain, the procedure is iterated. The $t\bar{t}$ mass is reconstructed from the lepton, the neutrino and the leading four jets or three jets (if only three jets remain). For events where there is a jet with a mass greater than 60 GeV, the hadronic top quark candidate is built combining this jet with closest jet in ΔR and the leptonic top quark candidate is built combining the reconstructed leptonically decaying W boson candidate with the closest jet, among the remaining jets. The $t\bar{t}$ mass spectrum is presented in Figure 1(a).

4.3 Boosted lepton plus jets channel

The $t\bar{t}$ system is reconstructed adding the four-momenta of the hadronically decaying top quark candidate, with the semileptonically decaying top quark candidate reconstructed from the leptonically decaying W boson candidate and the closest jet. The reconstructed $t\bar{t}$ mass spectrum is presented in Figure 1(b).

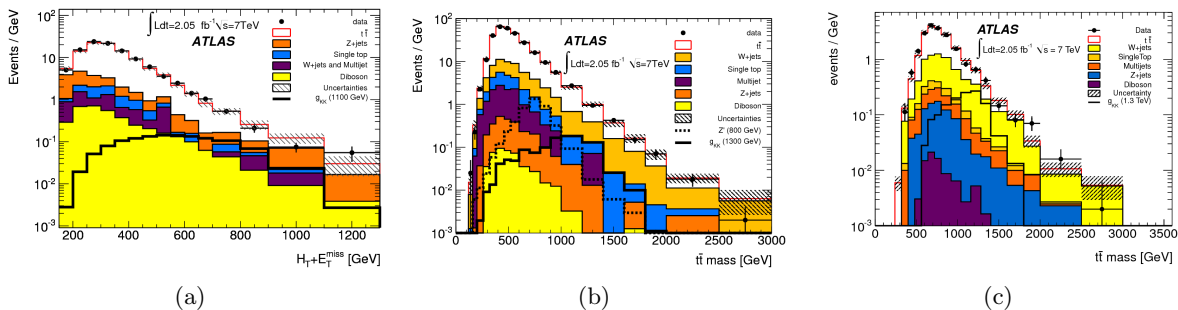


Figure 1: $H_T + E_T^{\text{miss}}$ distribution in the dilepton channel (a) and reconstructed $t\bar{t}$ mass in the lepton plus jets channel resolved (b) and boosted (c) after all the selection requirements. The hatched area shows the background normalization uncertainties^{3,4}.

5 Results

Figure 1 shows good agreement between data distributions and background expectations for the different discriminant variables used without visible evidence of a resonance structure above the expected backgrounds. Good agreement is seen in the shapes of kinematic distributions as well. The $t\bar{t}$ mass and $H_T + E_T^{\text{miss}}$ distributions are compared with the background-only and signal-plus-background hypothesis to verify that no statistically significant excess is observed. This was done using the BumpHunter²² tool for the lepton plus jets channels and a likelihood ratio test statistic for the dilepton channel. No significant excess was found. Given the absence of a new physics signal, limits were set using a Bayesian approach²³ (taking into account all the normalization and shape systematic uncertainties) on the cross-section times branching ratio as a function of mass. The predicted resonance cross-sections versus mass are used to convert the cross-section upper limits into mass limits.

For the dilepton channel, the observed (expected) limit for a Kaluza-Klein gluon in Randall-Sundrum models, g_{KK} , ranges from 18.5 (11.3) pb at $m_{g_{KK}} = 600$ GeV to 2.3 (2.7) pb at $m_{g_{KK}} = 1300$ GeV, excluding $m_{g_{KK}}$ between 500 (500) GeV and 1080 (1070) GeV at 95% CL. No mass limit is set on a narrow leptophobic topcolour Z' boson mass, $m_{Z'}$, since this channel has insufficient sensitivity to it. Limits on the g_{KK} production cross section time branching fraction are shown in Figure 2.

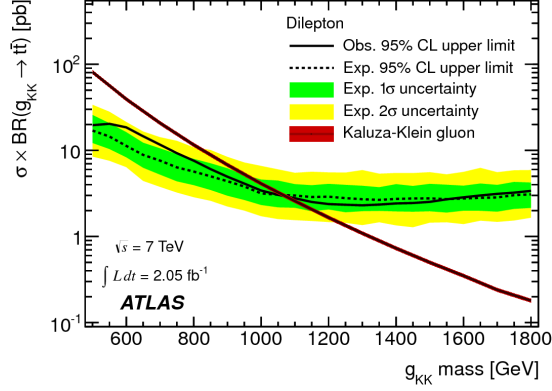


Figure 2: Observed (black points) and expected (dashed line) upper limits on $\sigma \times BR(Z' \rightarrow t\bar{t})$ (a) and $\sigma \times BR(g_{KK} \rightarrow t\bar{t})$ for the dilepton channel. The dark and light green bands show the range in which the limit is expected to lie in 68% and 95% of experiments, respectively².

For the lepton plus jets resolved channel, the observed (expected) limit for $\sigma \times BR(Z' \rightarrow t\bar{t})$ ranges between 4.8 (6.0) pb at $m_{Z'} = 600$ GeV and 0.95 (0.62) pb at $m_{Z'} = 1300$ GeV. The mass range $500 < m_{Z'} < 880$ GeV ($500 < m_{Z'} < 1010$ GeV) is excluded at 95% C.L. The observed (expected) limit for $\sigma \times BR(g_{KK} \rightarrow t\bar{t})$ ranges between 5.0 (6.0) pb at $m_{g_{KK}} = 500$ GeV and 1.6 (0.9) pb at $m_{g_{KK}} = 1300$ GeV. The mass range $500 < m_{g_{KK}} < 1130$ GeV ($500 < m_{Z'} < 1360$ GeV) is excluded at 95% C.L., as shown in Figure 3.

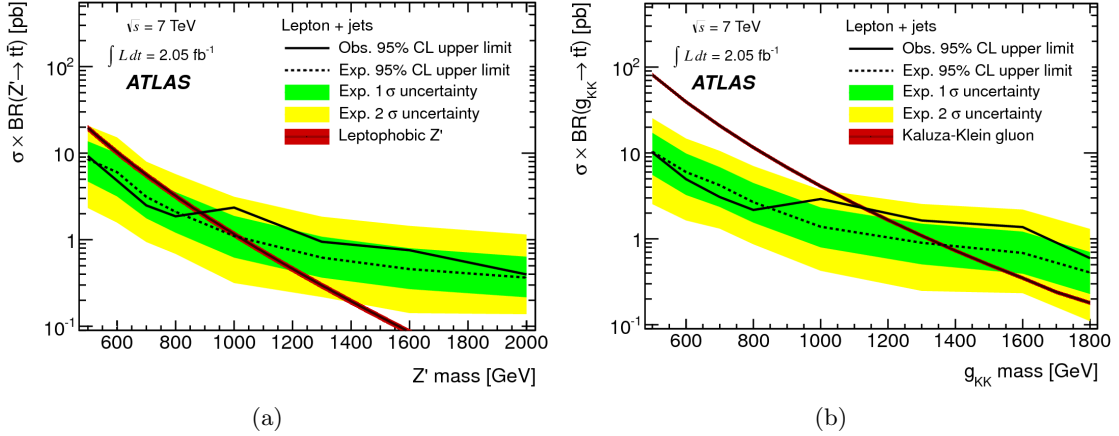


Figure 3: Observed (black points) and expected (dashed line) upper limits on $\sigma \times BR(Z' \rightarrow t\bar{t})$ (a) and $\sigma \times BR(g_{KK} \rightarrow t\bar{t})$ for the lepton plus jets resolved channel. The dark and light green bands show the range in which the limit is expected to lie in 68% and 95% of experiments, respectively².

For the lepton plus jets boosted channel, the observed (expected) limit for $\sigma \times BR(Z' \rightarrow t\bar{t})$ ranges between 7.7 (10.4) pb at $m_{Z'} = 600$ GeV to 0.56 (0.39) pb at $m_{Z'} = 1300$ GeV. The mass range between $600 < m_{Z'} < 1200$ GeV is excluded at 95% C.L. The observed (expected) limit for $\sigma \times BR(g_{KK} \rightarrow t\bar{t})$ ranges between 2.8 (2.9) pb at $m_{g_{KK}} = 700$ GeV to 0.8 (0.6) pb at $m_{g_{KK}} = 1300$ GeV. The mass range between $700 < m_{g_{KK}} < 1500$ GeV is excluded at 95% C.L.

6 Conclusion

Results of a search for $t\bar{t}$ resonances in the resolved lepton plus jets, boosted lepton plus jets and dilepton topologies have been presented. The different analyses use 2.05 fb^{-1} of pp collisions at $\sqrt{s} = 7$ TeV collected with the ATLAS detector in 2011. The data was compared to SM background prediction and found to be compatible within uncertainties. The $t\bar{t}$ mass ($H_T +$

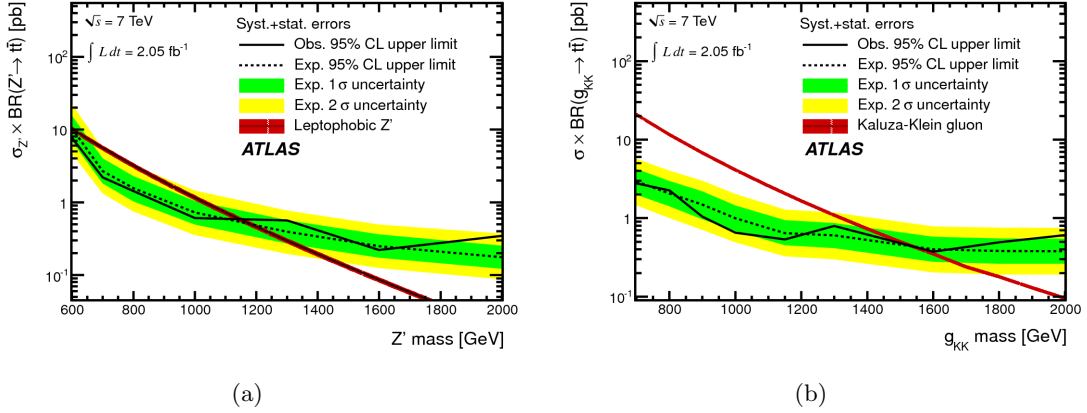


Figure 4: Observed (black points) and expected (dashed line) upper limits on $\sigma \times BR(Z' \rightarrow t\bar{t})$ (a) and $\sigma \times BR(g_{KK} \rightarrow t\bar{t})$ for the lepton plus jets boosted channel. The dark and light green bands show the range in which the limit is expected to lie in 68% and 95% of experiments, respectively ⁴.

E_T^{miss}) distribution in the lepton plus jets (dilepton) channels was used to set upper limits at 95% C.L. on the cross-section times branching ratio to $t\bar{t}$ of a narrow leptophobic topcolor Z' boson and a wide Kaluza-Klein gluon excitation g_{KK} in the Randall-Sundrum model. They exclude Z' bosons with masses between 500 and 1150 GeV and KK gluons with masses between 500 and 1500 GeV.

References

1. ATLAS Collaboration, *JINST* **3**, S08003 (2008).
2. ATLAS Collaboration, *Eur. Phys. J. C* **72**, 2083 (2012), arXiv:1205.5371.
3. ATLAS Collaboration, Tech. Rep. ATLAS-CONF-2012-029.
4. ATLAS Collaboration, *JHEP* **041**, 1209 (2012), arXiv:1207.2409.
5. R. M. Harris, C. T. Hill and S. J. Parke, *Phys. Lett. B* **345**, 483-489 (1995).
6. K. Agashe *et al.*, *Phys. Rev. D* **77**, 015003 (2008).
7. B. Lillie, J. Shu and T. M. P. Tait, *Phys. Rev. D* **76**, 115016 (2007).
8. B. Lillie, L. Randall and L.-T. Wang, *JHEP* **09**, 074 (2007), arXiv:hep-ph/0701166.
9. T. Aaltonen *et al.* (CDF Collaboration), *Phys. Rev. D* **84**, 072004 (2011).
10. M. Cacciari, G. P. Salam and G. Soyez, *JHEP* **04**, 063 (2008), hep-ph/0802.1189.
11. The ATLAS Collaboration, Accepted by *Eur. Phys. J.*(2011), arXiv:1112.6426.
12. ATLAS Collaboration, Tech. Rep. ATLAS-CONF-2011-102.
13. ATLAS Collaboration, *JHEP* **1205**, 128 (2012), arXiv:1203.4606.
14. S. Frixione and B. R. Webber, *JHEP* **06**, 029 (2002).
15. S. Frixione, P. Nason and B. R. Webber, *JHEP* **08**, 007 (2003).
16. G. Corcella *et al.*, *JHEP* **0101**, 010 (2001).
17. J. Butterworth, J. R. Forshaw and M. Seymour, *Z. Phys. C* **72**, 637 (1996).
18. ATLAS Collaboration, *Phys. Lett. B* **707**, 459 (2012).
19. M. L. Mangano *et al.*, *JHEP* **0307**, 001 (2003).
20. T. Sjostrand, S. Mrenna and P. Z. Skands, *JHEP* **0605**, 026 (2006).
21. J. Alwall *et al.*, *JHEP* **0709**, 028 (2007).
22. G. Choudalakis, arXiv:1101.0390 [physics.data-an].
23. I. Bertram *et al.* (DØ Collaboration), FERMILAB-TM-2104, Fermilab, 2000.